Temperature dependences of fluorescence lifetimes in Cr^{3+}-doped insulating crystals

Zhiyi Zhang, Kenneth T. V. Grattan, and Andrew W. Palmer
Department of Electrical, Electronic and Information Engineering, City University, Northampton Square, London, EC1V 0HB, United Kingdom
(Received 25 March 1993; revised manuscript received 3 June 1993)

The temperature dependences of the fluorescence lifetimes of Cr^{3+} doped insulating crystals, which have been used as temperature-sensing elements or have such potential uses for different temperature regions, are reviewed in terms of the crystal-field strength. Two single configurational coordinate models are proposed to interpret the temperature dependence of Cr^{3+} fluorescence in materials with low and high crystal-field strength. The validities of the two models are demonstrated by their close fit to the lifetime data of the Cr^{3+} fluorescence in appropriate materials. As was shown in thermometric applications, the expressions obtained for the temperature dependence of the fluorescence lifetimes, deduced from the proposed models, are of use as empirical calibration formulae in the assessment of various Cr^{3+} fluorescence lifetime-based thermometers.

I. INTRODUCTION

The properties of photoluminescence in materials, e.g., their comparative emission intensities at different wavelengths and their fluorescence lifetimes, exhibit strong temperature dependences over certain temperature regions. A high level of reproducibility of such temperature dependences is observed in many materials, and as a result such methods have gained thermometric applications in a number of optical sensor schemes.[1-6] Among them, those based on the monitoring of the fluorescence lifetimes of the photoluminescence in various rare-earth or transition-metal-ion activated luminescent species,[2-6] are much preferred in practical instruments, as the measurement of fluorescence lifetime is independent of a need for a precision measurement of light intensity and, consequently, the corresponding thermometers can be free of the need for repeated on-site calibrations. It is also one of the most successful practical schemes among the numerous existing fiber-optic temperature sensor methods proposed in the literature.[7]

The transition-metal ions, Cr^{3+}, are widely used as active dopants in solid-state laser crystals. Unlike rare-earth ions such as Nd^{3+}, Cr^{3+} ions in ionic crystals interact strongly with the crystal-field strength and the lattice vibrations. Thus, Cr^{3+} activated materials are characterized by a wide optical-absorption spectrum spanning the ultraviolet to the red portion of the visible spectrum. This allows the use of cheaper and compact light sources for excitation, such as high-power light-emitting diodes and visible laser diodes, highly suitable for practical sensor applications. Again due to the strong crystal-field interaction, the energy gaps of the electronic levels of Cr^{3+} ions vary from one host crystal to another, as do the temperature dependences of the fluorescence lifetimes of Cr^{3+}-doped materials. Therefore, significant variety in such temperature-dependent phenomena is observed and a useful level of control of this temperature dependence is made possible by systematic changes in the crystal-field strength, through the variation of the host material of the crystal composition, to cater to differing thermometric needs over various temperature regions.

The electronic energy levels of the Cr^{3+} ion are well illustrated by the Tanabe-Sugano diagram[8] which plots E/B, the normalized energy of the low-lying excited states as a function of the normalized octahedral crystal-field strength Dq/B. A simplified Tanabe-Sugano diagram is presented in Fig. 1 for a Cr^{3+} ion in an octahedral crystal field. The ground state is always the orbital singlet, $^4A_2$, irrespective of the strength of the octahedral crystal field. The energy splitting ΔE between the low-lying states, $^4T_2$ and ^2E, is defined as

$$\Delta E = E(^4T_2) - E(^2E) . \quad (1)$$

It varies strongly with Dq/B and may be positive or negative, as shown in Fig. 1. The broken lines indicate the energy-level positions of a number of different crystals. In a high strength crystal field, $Dq/B \gg 2.3$ as in ruby (Al_2O_3:Cr^{3+}) and alexandrite; $\Delta E > 0$ (2350 and ~ 800 cm^{-1} for ruby[9] and alexandrite,[10] respectively), and the Cr^{3+} emission is dominated by the sharp R lines

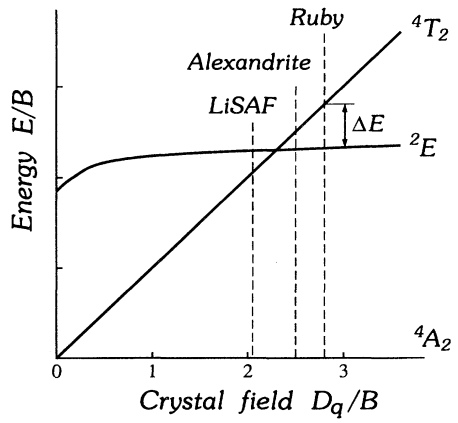

FIG. 1. A simplified Tanabe-Sugano diagram. The dashed lines represent the approximate energy-level positions of the Cr^{3+} ion in various host crystals.

($^2E \rightarrow {}^4A_2$ transition). However, by contrast in a low strength crystal field, $Dq/B \ll 2.3$, as in LiSAF ($LiSrAlF_6$); $\Delta E < 0$ and the dominant emission is the broad $^4T_2 \rightarrow {}^4A_2$ band transition. The change in the emission mechanism with a magnitude of Dq/B also gives the temperature dependence of the Cr^{3+} fluorescence lifetimes, showing different characteristics. Therefore, in the present study, the temperature dependences of the fluorescence lifetimes of Cr^{3+}-doped insulating crystals are reviewed in terms of the influence of the crystal-field strength.

II. TEMPERATURE DEPENDENCE OF Cr^{3+} FLUORESCENCE IN LOW-FIELD CRYSTALS

In a low crystal field, the lowest excited state is $^4T_2$. The ^2E state is less populated by the excited Cr^{3+} ions, according to the Boltzmann principle. Furthermore, due to the fact that the $^2E \rightarrow {}^4A_2$ transitions are doubly forbidden by parity and spin, these transitions are one or two orders of magnitude weaker than the $^4T_2 \rightarrow {}^4A_2$ transitions. Therefore, their impact on the fluorescence lifetime, which is mainly determined by the radiative and nonradiative processes of the $^4T_2 \rightarrow {}^4A_2$ transition in the material, is negligible. Its temperature dependence shares a similar profile to that of the fluorescence intensity, as demonstrated in Fig. 2 by the experimental data of the Cr^{3+} fluorescence in the laser crystal LiSAF ($LiSrAlF_6$), a low crystal-field material.

A single configurational coordinate model with only one excited state, as depicted in Fig. 3, could describe such temperature dependence qualitatively, and also quantitatively to the extent that it is adequate for the present thermometric applications, as will be shown later. The excited and ground states involved are $^4T_2$ and $^4A_2$, respectively. The $^4T_2 \rightarrow {}^4A_2$ transitions of the excited Cr^{3+} ions occur via two processes. One is the radiative transition initiated from I, the lowest energy point of the excited state. The other is a nonradiative process, that is the thermal quenching of the Cr^{3+} ions which have been

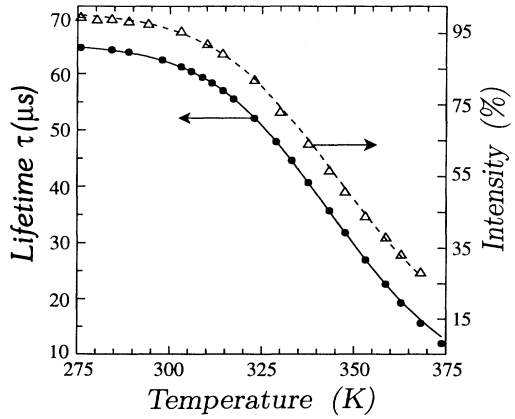

FIG. 2. Thermal characteristics of Cr^{3+} fluorescence in LiSAF. The solid circles denote the data on the fluorescence lifetimes; the open triangles denote the data on the fluorescence intensity.

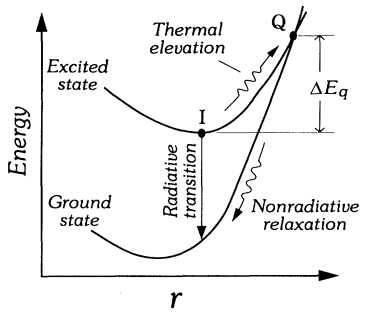

FIG. 3. Single configurational coordinate model for Cr^{3+} fluorescence in low-field crystals. r denotes the configurational coordinate.

thermally elevated to Q, the energy crossing of the excited and ground states and which will rapidly lose energy to reach the bottom of the ground state through nonradiative relaxation, as indicated schematically in Fig. 3. The two processes are continuously competing with each other. The higher the temperature, the more excited ions will be elevated to the level crossing Q, and the stronger the nonradiative process will be. Normally the nonradiative transitions are much faster. Therefore, the $^4T_2 \rightarrow {}^4A_2$ transition rates increase with elevated temperature, and a decrease of fluorescence lifetimes with temperature increase is observed.

According to this model $1/\tau$ the transition rate of Cr^{3+} in the excited state may be given by

$$1/\tau = 1/\tau_i + (1/\tau_q) e^{-\Delta Eq/kT} , \tag{2}$$

where τ is the observed fluorescence lifetime, $1/\tau_i$ is the intrinsic radiative rate at the excited state, $1/\tau_q$ is the thermal quenching rate, ΔE_q is the thermal activation needed to elevate ions at the bottom of the excited state to the level crossing Q, k is the Boltzmann constant, T is the absolute temperature and, thus, $e^{-\Delta Eq/kT}$ represents the possibility of the excited ions being elevated to the energy corresponding to the crossing of the levels Q. On the assumption that the output power and spectral characteristics of the excitation light source, as well as the absorbance of the luminescent sample over the corresponding spectrum are constant over the temperature region concerned, the observed fluorescence intensity may be expressed as

$$I = \frac{I_0}{1+\beta e^{-\Delta Eq/kT}} , \tag{3}$$

where I_0 is a constant determined by the excitation scheme used and

$$\beta = \tau_i/\tau_q . \tag{4}$$

To obtain a direct expression of the fluorescence lifetime, Eq. (2) may be rewritten as

$$\tau = \frac{\tau_i}{1+\beta e^{-\Delta Eq/kT}} . \tag{5}$$

It is clearly shown in Eqs. (3) and (5) that the temperature

TABLE I. Empirical values of parameters in the configurational coordinate model of Cr:LiSAF fluorescence.

	$\ln\beta$	ΔE_q (cm^{-1})	τ_i (μs)
Values fitted to the lifetime data	18.89	4557	62.25
Values fitted to the intensity data	18.70	4533	

dependences of the fluorescence intensity and lifetime are similar.

The Cr^{3+}-doped LiSAF is a recently developed laser crystal.[11,12] Its crystal-field strength, estimated from the spectroscopic data obtained by Payne, Chase, and Wilke,[12] is of the order of $Dq/B=2.0$. In the previous work of the authors,[13] it has been shown successfully for use in a fiber-optic thermometer for the monitoring of temperature in clinical rf heat treatment. To predict performance in such an application, Eqs. (3) and (5) are used in a fit of the experimental data of Cr:LiSAF fluorescence plotted in Fig. 2 and the results are depicted as dashed and solid lines, respectively. The standard deviation for Eq. (5) to fit the Cr:LiSAF fluorescence lifetime data over the region 300–353 K is 0.12%, representing a very close agreement. The fitted values of ΔE_q and β as well as τ_I are listed in Table I. The differences between these values, fitted to the lifetime and intensity data, respectively, for $\ln\beta$ and ΔE_q are only of the order of 1%. These verify that the lifetime and intensity of Cr^{3+} fluorescence in LiSAF have the same temperature dependence, a conclusion also obtained from the configurational coordinate model in Fig. 3.

Two other crystal materials, LiBAF ($LiBaAlF_6$) and LiCAF ($LiCaAlF_6$) are similar to LiSAF in chemical structure, and are also of low crystal-field strength. From the spectroscopic data obtained by Stalder, Chai, and Bass[14] and Payne, Chase, and Wilke,[12] their crystal-field strengths Dq/B are also of the order of 2.0. The temperature dependences of Cr^{3+} fluorescence lifetimes in LiBAF and LiCAF are plotted in Fig. 4 according to the experimental data from Stalder, Chai, and Bass,[14] together with that in LiSAF. As shown by these examples, the fluorescence lifetimes of Cr^{3+} in the low crystal field are

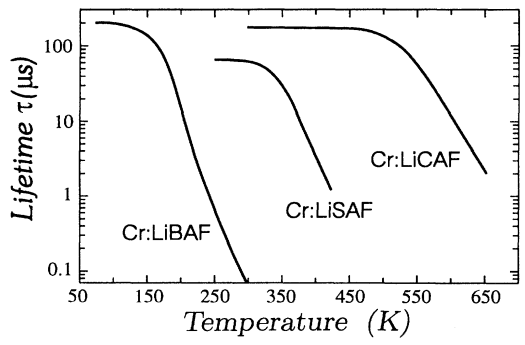

FIG. 4. Temperature dependences of the fluorescence lifetimes of Cr:LiBAF, Cr:LiCAF (Ref. 14), and Cr:LiSAF.

particularly sensitive to temperature variance over a limited temperature region. This characteristic makes the low-field crystal materials quite suitable for thermometric applications where high measurement resolution is required over a relative narrow region of temperature, and thus the observation that low-field crystal materials can cater to such applications over various temperature regions. Typically, for measurements in the biomedical region, as in the application mentioned before, the temperature dependence of the Cr:LiSAF fluorescence lifetime is most useful. Those of the Cr:LiBAF and Cr:LiCAF fluorescence lifetimes have the potential for applications over the cryogenic region, 100–250 K, and the higher temperature region, 470–650 K, respectively. Thus, the effective upper limits of thermometric use may be different from the data produced. This is normally much higher for doped thermometric crystal materials than for doped glasses (e.g., a study of Nd^{3+}-doped materials[15]).

III. TEMPERATURE DEPENDENCE OF Cr^{3+} FLUORESCENCE IN HIGH-FIELD CRYSTALS

In the high strength crystal field ($Dq/B \gg 2.3$), the lowest excited state of Cr^{3+} is ^2E. At low temperatures, the Cr^{3+} luminescence is dominated by $^2E \rightarrow {}^2A_4$ transitions so that long fluorescence lifetimes are observed, e.g., ~ 1.5 ms at 100 K for alexandrite[10] and ~ 3.5 ms at 300 K for ruby. With increasing temperature, a higher percentage of the excited Cr^{3+} ions will populate the short lifetime $^4T_2$ state and consequently, more $^4T_2 \rightarrow {}^2A_4$ transitions will be initiated, which results in a decrease of the fluorescence lifetimes. Thus, at lower temperatures, the temperature dependence of the Cr^{3+} fluorescence lifetimes is dominated by the thermally activated repopulation between the excited ^2E and $^4T_2$ states. At even higher temperatures, a higher level of nonradiative transitions appears which will significantly speed up the decrease in the fluorescence lifetimes. In this section, a discussion of a two-level model is undertaken, describing the temperature dependence of the fluorescence lifetimes due to the thermally activated repopulation between the ^2E and $^4T_2$ states at lower temperatures. This is developed to take account of both the thermally activated repopulation mentioned above and the nonradiative process, where a single configurational coordinate model with two excited levels is presented for the temperature dependence over the whole region studied.

A. Two-level model for the Cr^{3+} fluorescence in high fields

At lower temperatures, where the nonradiative transitions of the excited Cr^{3+} ions back to the ground state are negligible, the temperature dependence of the Cr^{3+} fluorescence in high crystal fields can adequately be described by a two level model, which has been used by Walling *et al.*[10] in the case of alexandrite ($BeAl_2O_4:Cr^{3+}$) laser action, as shown in Fig. 5. Due to the long lifetime of the ^2E state, at elevated temperatures, most radiative transitions will initiate from the $^4T_2$ state and ^2E functions more as a store of the excited ions; thus it is termed

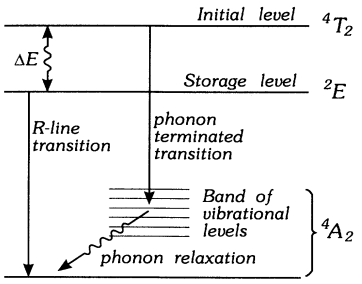

FIG. 5. The two-level model for Cr^{3+} fluorescence in high-field crystals.

here the "storage level." The assumption that the $^4T_2$ and ^2E are in "quasithermodynamic equilibrium" with one another can be made, and this is verified for ruby and alexandrite where the upper limits of the nonradiative relaxation times for the $^4T_2 \rightarrow {}^2E$ transition are 7 ps for ruby and 27 ps for alexandrite, respectively.[16,17] Thus, by taking account of the degeneracies of the $^4T_2$ and ^2E states, a mathematical expression for the fluorescence lifetimes as a function of temperature can be deduced from the two-level model as the following:

$$\tau=\tau_s\frac{1+C_d e^{-\Delta E/kT}}{1+(\tau_s/\tau_i)e^{-\Delta E/kT}}=\tau_s\frac{1+3e^{-\Delta E/kT}}{1+\alpha e^{-\Delta E/kT}}\ , \tag{6}$$

where τ is the fluorescence lifetime, ΔE is the energy gap between the $^4T_2$ and ^2E states as defined in Eq. (1), τ_i and τ_s are the lifetimes of the $^4T_2$ and ^2E states, and C_d is the ratio of the degeneracy of $^4T_2$ to that of ^2E, with a value of 3.

The temperature dependences of alexandrite fluorescence are depicted in Fig. 6, where the open triangles represent the fluorescence lifetime data from Walling *et al.*[10] over the region 4–500 K and the solid circles the data over the 290–940-K region obtained by the authors, as described in previous work.[18] The solid line is the least-squares fit of Eq. (6) to the fluorescence lifetime data obtained by the authors, ranging from 290 to 680 K. It shows that Eq. (6) fits the fluorescence lifetime data quite well over the region 200–700 K. The fitted values of the parameters in Eq. (6), are listed in Table II. According to the spectroscopic data obtained by Suchocki *et al.*,[19] the energy difference between the lowest members of the $^4T_2$ and ^2E states is 807.5 cm^{-1} at 12 K. The fitted value of ΔE is rather close to this spectroscopic value. The value of τ_s was measured by Walling *et al.*[10] to be 1.32 ms at 4 K (for the mirror site). Though based on data beyond a temperature of 290 K, the observed value of τ_s fits to the above value quite well. In earlier work,[20] ΔE and τ_s were fitted to be $\sim$750 cm^{-1} and 2.52 ms, where the difference between the $^4T_2$ and ^2E states in degeneracies was neglected, that is, the value of C_d in Eq. (6) was taken as 1. Here, based on the same data, a much closer fit is achieved by taking account of the degeneracy difference.

As shown in Fig. 6, there are two temperature regions where the discrepancy between the fluorescence lifetime data and the fitted curve is quite significant. One is from 4 K to $\sim$200 K over which the discrepancy is due to the rise in lifetime with increasing temperature between 4 and 70 K caused by thermal excitation in excited ions from the lower ^2E to the longer lifetime upper ^2E level.[10] Over this region, the relationship between the fluores-

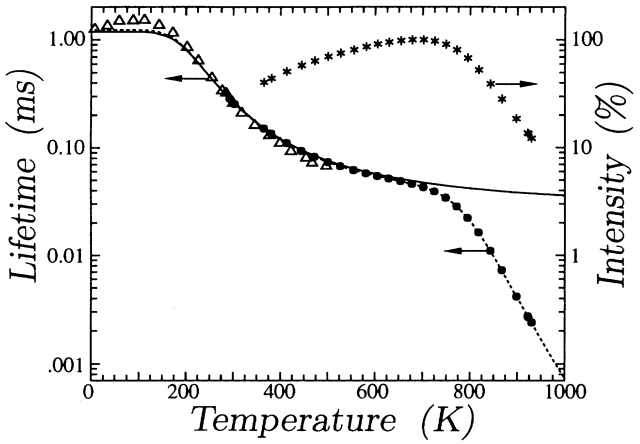

FIG. 6. Temperature dependence of the alexandrite fluorescence. The solid circles denote the fluorescence lifetime data taken by the authors; the asterisks denote data for the fluorescence intensity of the broadband vibronic emission ($> \sim$690 nm) induced by a 662-nm diode laser; the solid line denotes the least-squares curve of Eq. (6) fitted to the fluorescence lifetime data over the region 290–680 K; the dashed line denotes the least-squares curve of Eq. (10) fitted to the lifetime data from 300 to 930 K; the open triangles denote the fluorescence lifetime data from Walling *et al.* (Ref. 10).

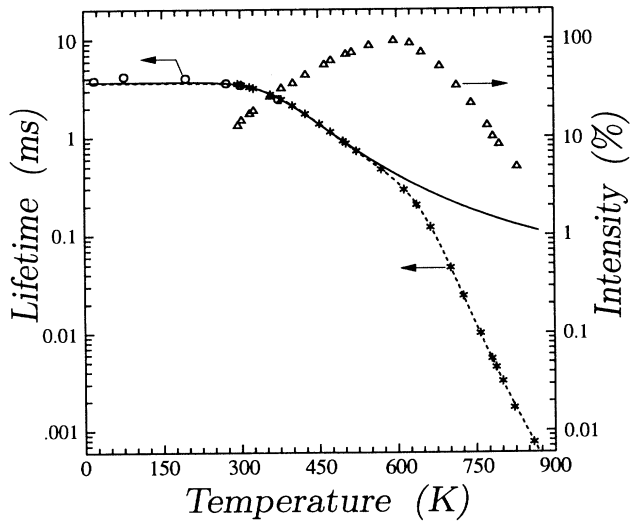

FIG. 7. Temperature dependence of the ruby fluorescence. The asterisks denote the fluorescence lifetime data where a HeNe laser (633 nm) is used as the excitation source; the open triangles denote the data for the fluorescence intensity at the broadband emission ($>$695 nm); the solid line denotes the least-squares curve of Eq. (6) fitted to the fluorescence lifetime data over the region 300–475 K; the dashed line denotes the least-squares curve of Eq. (10) fitted to the lifetime data from 300 to 800 K; the open circles denote the lifetime data from Nelson and Sturge (Ref. 21).

cence lifetime and the temperature is not monotonic, so it has little thermometric use. For the same reason, such a region also exists in the case of ruby, as shown in Fig. 7 from 20 K to ~275 K, where the solid line represents the least-squares curve of Eq. (6) fitted to the lifetime data ranging from 300 to 570 K.

The other region over which the fluorescence lifetime decreases sharply with increasing temperature is beyond ~700 K. The decrease in the fluorescence intensity over the broadband emission with increasing temperature beyond this temperature, as shown in Fig. 7, reveals that the discrepancy of the two-level model with the experimental data over this region is due to the nonradiative transitions which are becoming stronger with increasing temperature beyond ~700 K. Again, the same phenomenon can be observed in ruby at a lower temperature (beyond ~600 K), as illustrated in Fig. 7. The nonradiative transitions accelerate the decrease in the fluorescence lifetime with increasing temperature, and make the fluorescence lifetime much more sensitive to temperature variance at high temperatures.

B. The configurational coordinate model for the Cr^{3+} fluorescence in high fields

To include the effect of the nonradiative transitions, a single configurational coordinate model redrawn in Fig. 8, has been used by the authors[20] in the case of alexandrite. According to this model, the change of the total population of the $^4T_2$ and ^2E states, n is described by the rate equation

$$\frac{dn}{dt}=-(1/\tau_s)n_s-[1/\tau_i+(1/\tau_q)e^{-\Delta Eq/kT}]n_i \ , \quad (7)$$

where n_s and n_i are the populations of ^2E and $^4T_2$, respectively; $1/\tau_s$, $1/\tau_i$ and $1/\tau_q$, ΔE_q are as defined in Eq. (6). On the assumption that the $^4T_2$ and ^2E are in "quasithermodynamic equilibrium" with one another, that is,

$$\frac{n_i}{n_s}=C_d e^{-\Delta E/kT} \ , \quad (8)$$

where $C_d=3$, as defined in Eq. (6), the rate equation may be rewritten as

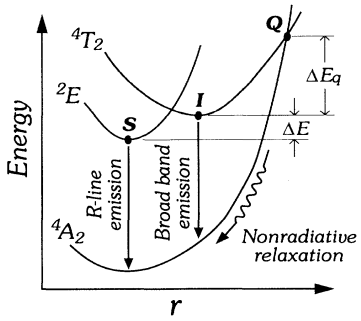

FIG. 8. The single configurational coordinate model for Cr^{3+} fluorescence in high-field crystals. r denotes the configurational coordinate.

TABLE II. Empirical values of parameters in appropriate models, fitted to the alexandrite fluorescence lifetime data.

	ΔE (cm^{-1})	τ_s (ms)	$\ln\alpha$
Spectroscopic data	807.5[a]	1.32[b]	
Two-level model (290–650 K)	857.0	1.17	5.40
Configurational coordinate model (290–930 K)	18.70	1.23	5.44

[a]Suchocki *et al.* (Ref. 19).
[b]Walling *et al.* (Ref. 10).

$$\frac{dn}{dt}=-\frac{1/\tau_s+(1/\tau_i)e^{-\Delta E/kT}+(1/\tau_q)e^{-(\Delta Eq+\Delta E)/kT}}{1+3e^{-\Delta E/kT}}n \ . \quad (9)$$

Therefore, the fluorescence lifetime τ is given by

$$\tau=\tau_s\frac{1+3e^{-\Delta E/kT}}{1+\alpha e^{-\Delta E/kT}+\beta e^{-(\Delta Eq+\Delta E)/kT}} \ , \quad (10)$$

where $\alpha=\tau_s/\tau_i$ and $\beta=\tau_s/\tau_q$. The dashed line in Fig. 6 is the least-squares fitting of Eq. (10) to the lifetime data from 290 to 930 K for alexandrite. The fitted values for ΔE, τ_s, and $\ln\alpha$ are listed in Table II as a comparison to those fitted by using the two-level model, and the values for ΔE_q and $\ln\beta$ are fitted to be 10 807 cm^{-1} and 24.8, respectively. In this approximation, the samples used are separated by a temperature interval of ~20 K. The standard deviation of the relative fitting errors of the lifetimes is ~0.3%. Equation (10) has also been applied to fit the lifetime data of ruby presented in Fig. 7 from 300 to 800 K. The fitted curve is depicted as the dashed line in the same figure. The deviation of the curve fitting is ~1%.

C. Other contributions to temperature dependence at low temperatures

At sufficiently low temperatures, e.g., $T<\Delta E/(k\ln\alpha)$ (that is, $T<400$ K for ruby and $T<200$ K for alexandrite), contributions other than those from the thermalization between the $^4T_2$ and ^2E states will have a significant effect upon the temperature dependence of the Cr^{3+} fluorescence lifetime in a high strength field, as will be shown in the case of ruby. The illustration of the temperature dependence of ruby fluorescence lifetime, presented in Fig. 7, is magnified at low temperatures in Fig. 9. The solid line is the least-squares fit of the two-level model, expressed in Eq. (6), to the fluorescence data ranging from ~300 to 500 K, denoted by the solid circles. The corresponding fitted values of the parameters in Eq. (6) are listed in Table III. The fitted value of ΔE differs from the spectroscopic value, 2350 cm^{-1}, by ~17%. Due to the size of this discrepancy, it would be expected that other mechanisms are involved in the determination of the temperature dependence. Also, the increase in the fluorescence lifetime with increasing temperature at even lower temperatures, $T<\sim100$ K, as observed in ruby and alexandrite, could not be interpreted

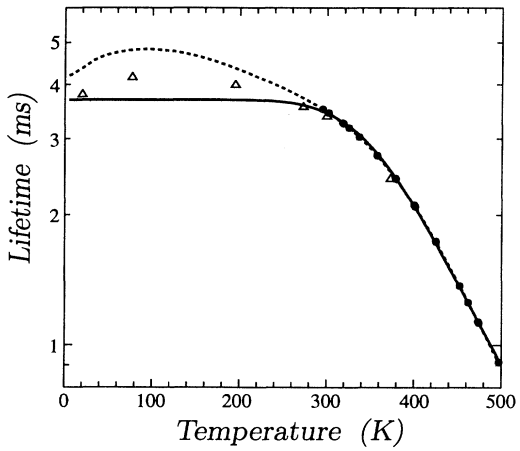

FIG. 9. Temperature dependence of ruby fluorescence lifetime over a lower temperature band, to 500 K. The open triangles denote data from Nelson and Sturge (Ref. 21).

in a satisfactory way by the two-level model.

As clearly identified by Fonger and Struck[9] from the phonon sidebands of the ruby $^2E \rightarrow {}^4A_2$ emission at 77 K, there are two prominent phonon energies given by

$$h\nu_1 = 430 \text{ cm}^{-1}, \quad h\nu_2 = 280 \text{ cm}^{-1}. \tag{11}$$

The ratio of the peak intensity of the sidebands corresponding to these two phonon energies $I(h\nu_1)/I(h\nu_2)$ is ~ 0.65. The contribution of the phonon-induced transitions to the temperature dependence results in an increase in emission probability by a factor of $\coth(h\nu/2kT)$.

In addition, the ^2E state is further split into $\bar{E}$ and $2\bar{A}$ states by a tiny energy gap of $\Delta E_R = 29.1 \text{ cm}^{-1}$ in ruby, which results in two sharp R-line emissions, R_1 (693.4 nm, $\bar{E} \rightarrow {}^4A_2$) and R_2 (692.8 nm, $2\bar{A} \rightarrow {}^4A_2$), familiar in the ruby laser. At temperatures close to $\Delta E_R/k$ or below, the thermalization between the $\bar{E}$ and $2\bar{A}$ states will dominate the temperature dependence of the fluorescence lifetime. Due to the longer radiative lifetime of the high-lying $2\bar{A}$ state, this gives rise to the increase in fluorescence lifetime with increasing temperature over certain parts of the "cryogenic region," as demonstrated by the temperature dependences of alexandrite and ruby fluorescence lifetimes below 100 K. It has been verified in the work of Weinstein[22] that such thermalization in ruby can be adequately described by simple Boltzmann statistics over the region 0–100 K as

$$I_{R2}/I_{R1} = \alpha_R e^{-\Delta E_R/kT}, \tag{12}$$

where I_{R1}, I_{R2} are intensities of R_1 and R_2 emission, respectively, and the ratio α_R is found to be

$$\alpha_R = 0.65. \tag{13}$$

Therefore, to describe closely the overall temperature dependence of the Cr^{3+} fluorescence lifetime at low temperatures, the two-level model expressed by Eq. (6) has to be modified to take account of the phonon-induced transitions and the splitting of the ^2E state. Thus, in the case of ruby, by assuming that the R-line phonon sidebands induced by $h\nu_1$ and $h\nu_2$ originate from R_1 and R_2 emission, respectively, the two-level model may be modified according to the following expression:

$$\tau = \tau_s \frac{1 + e^{-\Delta E_R/kT} + 6e^{-\Delta E/kT}}{\coth(h\nu_1/2kT) + \alpha_R \coth(h\nu_2/2kT) e^{-\Delta E_R/kT} + \alpha e^{-\Delta E/kT}}, \tag{14}$$

where $\Delta E_R = 29.1 \text{ cm}^{-1}$; and the values of $h\nu_1$, $h\nu_2$, and α_R are given in Eqs. (11) and (13), respectively. The values of ΔE, τ_s, and $\ln\alpha$ obtained by a least-squares fit to the ruby fluorescence lifetime data ranging from ~ 300 to 500 K are listed in Table III. Not only does this modified model fit the lifetime data much better, with a standard deviation of 0.14%, compared to that of 0.77% achieved by the previous model, but also the value of ΔE resulting from the using of this model agrees with the spectroscopic data quite well, as shown in Table III. The corresponding least-squares curve is depicted as the dashed line in Fig. 9.

TABLE III. Empirical values of parameters in appropriate models, fitted to the ruby fluorescence lifetime data ranging from ~ 300 to 500 K.

	ΔE (cm^{-1})	τ_s (ms)	$\ln\alpha$	σ_n (%)
Spectroscopic data[a]	2350			
Two-level model	1957	3.69	6.76	0.77
Modified two-level model	2351	4.20	8.53	0.14

[a]Data from Fonger and Struck (Ref. 9).

IV. DISCUSSION

It has been seen that the temperature dependence of the Cr^{3+} fluorescence is strongly characterized by the crystal-field strength. Furthermore, the degree of variation of the fluorescence lifetime with temperature can indicate whether the field strength of the host material is high or low. In a host with a low crystal field, the decrease in the Cr^{3+} fluorescence lifetime with increasing temperature changes rapidly only over one continuous temperature region, as is observed, e.g., from ~ 300 to ~ 400 K in LiSAF. However, in a high-field host, two

such regions are found. For instance, in alexandrite, such regions range from ~150 to ~300 K and from ~700 K and beyond; in ruby, from ~300 to ~500 K and from ~600 K and beyond.

Two configurational coordinate models, presented in Figs. 3 and 8, are sufficient to allow the interpretation of the temperature dependences of the Cr^{3+} fluorescence in crystal materials qualitatively, even quantitatively to an extent of sufficient precision for thermometric applications, as shown in the cases of Cr:LiSAF, alexandrite, and ruby. In high-field strength host crystals, two mechanisms, the thermal repopulation of the $^4T_2$ and ^2E states and the nonradiative process dominate the temperature dependence alternately over different temperature regions. Thus, the fluorescence lifetimes are quite sensitive to temperature variances over a wide temperature region, and are suitable for wide range thermometric uses. In addition, the total fluorescence efficiency does not decrease with increasing temperature over the region where the thermal repopulation of the $^4T_2$ and ^2E states dominates, and an increase in absorption of the excitation light is observed, as in alexandrite.[20]

By contrast, in Cr^{3+}-doped low-field crystals, partly due to the lower degree of overlapping between the absorption and emission spectra, compared with that in high-field crystals, the self-trapping of fluorescence is rather weak. In some low-field crystals, the dependence of the fluorescence lifetime on the Cr^{3+} concentration is rather slight even up to very high concentrations, e.g., from 2% to 15% for Cr:LiSAF (Ref. 23) and from 1% to 10% for Cr:LiBAF.[14] These properties indicate that slight changes in the Cr^{3+} concentration of the samples used in the thermometers, the size, and the positioning of the sample materials in the formation of the temperature probes, will have no significant effect on the measurements. As a result, the measurement reproducibility and the exchangeability of the temperature probes using the same sensing materials will be greatly enhanced.

[1]R. V. Alves, J. Christol, M. Sun, and K. A. Wickersheim, Adv. Instrum. **38**, 925 (1983).
[2]R. R. Sholes and J. G. Small, Rev. Sci. Instrum. **51**, 882 (1980).
[3]T. Bosselmann, A. Reule, and J. Schröder, Proc. SPIE **514**, 151 (1984).
[4]K. Wickersheim, S. O. Heineman, H. N. Tran, and M. H. Sun, in *Northeastern Conference on Industrial Instrumentation and Control, Boston, 1984,* Proceedings of Digitech '85 (Instrument Society of America, Boston, 1985), pp. 87–94.
[5]K. T. V. Grattan and A. W. Palmer, Rev. Sci. Instrum. **56**, 1784 (1985).
[6]K. T. V. Grattan, R. K. Selli, and A. W. Palmer, Rev. Sci. Instrum. **59**, 1328 (1988).
[7]K. T. V. Grattan, in *Fiber Optic Chemical Sensors and Biosensors,* edited by. O. S. Wolfbeis (CRC, London, 1991), Vol. II, Chap. 15, pp. 151–192.
[8]S. Sugano, Y. Tanabe, and H. Kamimura, *Multiplets of Transition-Metal Ions in Crystals* (Academic, New York, 1970), pp. 107–112.
[9]W. H. Fonger and C. W. Struck, Phys. Rev. B **11**, 3251 (1975).
[10]J. C. Walling, O. G Peterson, H. P. Jenssen, R. C. Morris, and E. W. O'Dell, IEEE J. Quantum Electron. **QE-16**, 1302 (1980).
[11]S. A. Payne, L. L. Chase, L. K. Smith, W. K. Kway, and H. W. Newkirk, J. Appl. Phys. **66**, 1051 (1989).
[12]S. A. Payne, L. L. Chase, and G. D. Wilke, J. Lumin. **44**, 167 (1989).
[13]Z. Y. Zhang, K. T. V. Grattan, and A. W. Palmer, Proc. SPIE **1885**, 228 (1993).
[14]M. Stalder, B. H.T. Chai, and M. Bass (unpublished).
[15]K. T. V. Grattan, J. D. Manwell, S. M. L. Sim, and C. A. Willson, Opt. Commun. **62**, 104 (1987).
[16]S. K. Gayen, W. B. Wang, V. Petricevic, R. Dorsinville, and R. R. Alfano, Appl. Phys. Lett. **47**, 455 (1985).
[17]S. K. Gayen, W. B. Wang, V. Petricevic, and R. R. Alfano, Appl. Phys. Lett. **49**, 437 (1986).
[18]Z. Y. Zhang, K. T. V. Grattan, and A. W. Palmer, Rev. Sci. Instrum. **63**, 3869 (1992).
[19]A. B. Suchocki, G. D. Gilliland, R. C. Powell, J. M. Bowen, and J. C. Walling, J. Lumin. **37**, 29 (1987).
[20]Z. Y. Zhang, K. T. V. Grattan, and A. W. Palmer, J. Appl. Phys. **73**, 3493 (1993).
[21]D. F. Nelson and M. D. Sturge, Phys. Rev. **137**, A1117 (1965).
[22]B. A. Weinstein, Rev. Sci. Instrum. **57**, 910 (1986).
[23]M. Stalder, B. H. T. Chai, and M. Bass, Appl. Phys. Lett. **58**, 216 (1991).